The Effects of Chemical Additives on the Induction Phase in Solid-State Thermal Decomposition of Ammonia Borane

David J. Heldebrant,[†] Abhi Karkamkar,[†] Nancy J. Hess,[†] Mark Bowden,[‡] Scot Rassat,[†] Feng Zheng,[†] Kenneth Rappe,[†] and Tom Autrey*,[†]

Pacific Northwest National Laboratory, P.O. Box 999, Richland, Washington 99352, and Industrial Research Limited, Lower Hutt, New Zealand

Received May 9, 2008. Revised Manuscript Received June 13, 2008

The thermal decomposition of ammonia borane (AB) in the absence and presence of chemical additives was investigated to develop an approach for reducing the induction period for hydrogen release in the solid state. Gas chromatography techniques were used to measure the yield of hydrogen as a function of time under isothermal conditions between 75 and 90 °C to set the baseline. Solid-state ^{11}B-NMR spectroscopy of the products produced after 1 mol equiv of hydrogen had been desorbed from AB (i.e., polyaminoborane) showed a complex mixture of sp^3 boron species. Raman microscopy was used to follow the transformation of crystalline AB to amorphous AB upon heating and the subsequent formation of the diammoniate of diborane (DADB). A gas buret was used to monitor the time-dependent release of hydrogen from AB in the presence of chemical additives. The combination of these approaches provides insight into the mechanism of hydrogen release from solid AB. The release of molecular hydrogen is described by a process involving sequential induction (disruption of dihydrogen bonds), nucleation (formation of DADB), and growth (hydrogen release through dehydrocoupling). Addition of DADB or ammonium chloride to neat AB significantly reduces the induction time for hydrogen release. These results provide approaches to improve the hydrogen storage properties of AB.

Introduction

Interest in alterative energy sources is growing as concerns over greenhouse gas emissions and the demand for finite quantities of conventional oil-based fuel sources are escalating. The potential advantages of a "hydrogen economy" are far reaching, ranging from the promise of an environmentally clean energy source, through the use of renewable fuels, to an enhanced energy security for the nation. If we are to successfully transition our energy economy from oil-based to hydrogen-based, we must engage in research and development to increase the efficiency and lifetime of fuel cells, decrease the costs of hydrogen production, and discover new materials that can store adequate volumetric and gravimetric quantities of hydrogen, especially for on-board fuel cells used in vehicular applications.

Given its high gravimetric density of 19 wt % hydrogen, AB, a solid molecular crystal, has received considerable attention recently as a potential hydrogen storage material.[1] Until recently, little has been reported on the optimum reaction conditions and important pathways for releasing hydrogen from solid AB. Thermal analysis by Hu and co-workers reported that hydrogen is released from AB vigorously at temperatures above the melting point.[2] To the best of our knowledge, Wolf and co-workers were the first to have investigated the potential of AB as a hydrogen-storage medium for fuel-cell-powered vehicles.[3] They showed that heating solid AB to temperatures between 70 and 90 °C results in the release of one molar equivalent of hydrogen gas and a complex polymeric aminoborane (PAB), albeit at slow rates because of the long induction period prior to hydrogen release.[4] Recently, considerable effort has been directed at enhancing hydrogen release from AB. We reported the effect of scaffolds, such as mesoporous silica SBA-15 and carbon cryogels, to enhance the hydrogen-release properties of AB.[4] Sneddon and co-workers[5] showed that ionic liquids facilitate hydrogen release from AB, while others have shown that acid catalysts promote hydrogen release in aqueous media[6,7] and organic solvents.[8,9] Benedetto et al.[10] have shown that mechanical activation such as ball milling with metal catalysts enhances hydrogen release in solid state AB. However, all of these approaches either contribute excess weight and volume to the storage system or require expensive precious metal catalysts. Unfortunately the rate of hydrogen release from solid-state AB in the

* Corresponding author. E-mail: tom.autrey@pnl.gov.
† Pacific Northwest National Laboratory.
‡ Industrial Research Limited.

(1) Marder, T. *Angew. Chem., Int. Ed.* **2007**, *46*, 8116–8118.
(2) Hu, M.; Geanangel, R.; Wendlandt, W. *Thermochim. Acta* **1978**, *23*, 249.
(3) Wolf, G.; Baumann, J.; Baitalow, F.; Hoffmann, F. *Thermochim. Acta* **2000**, *243*, 19.
(4) Gutowska, A.; Li, L.; Shin, Y.; Wang, C.; Li, X.; Linehan, J.; Smith, R.; Kay, B.; Schmid, B.; Shaw, W.; Gutowski, M.; Autrey, T. *Angew. Chem. Int. Ed.* **2005**, *44*, 3578–3582.
(5) Bluhm, M.; Bradley, M.; Butterick, R.; Kusari, U.; Sneddon, L. *J. Am. Chem. Soc.* **2006**, *128*, 7748–7749.
(6) Chandra, M.; Xu, Q. *J. Power Sources* **2006**, *156*, 190–194.
(7) Yan, J. M.; Zhang, H. B.; Han, S.; Shioyama, H.; Hu, Q. *Angew. Chem., Int. Ed.* **2008**, *47*, 2287–2289.
(8) Stephens, F.; Baker, R.; Matus, M.; Grant, D.; Dixon, D. *Angew. Chem. Int. Ed.* **2007**, *46*, 746–749.
(9) Clark, T.; Manners, I. *J. Organomet. Chem.* **2007**, *692*, 2849–2853.
(10) De Benedetto, S.; Carewska, M.; Cento, C.; Gislon, P.; Pasquali, M.; Scaccia, S.; Paolo Prosini, P. *Thermochim. Acta* **2006**, *441*, 184.

10.1021/cm801253u CCC: $40.75
Published on Web 08/02/2008

absence of a catalyst is limited at these lower temperatures by a long induction period of several minutes at 90 °C and up to several hours at 70 °C. We have been interested in mechanistic pathways that lead to hydrogen release from solid-state AB, especially the phenomena occurring during the long induction period leading to the nucleation process required to initiate hydrogen release. We recently reported findings from in situ X-ray diffraction (XRD) and optical microscopy studies that suggest there is a disruption of the dihydrogen bonding in AB during the induction period occurring at temperatures between 75 and 90 °C.[11] The loss of crystallinity observed in the XRD diffractograms supports the conclusions of a recent in situ ^{11}B NMR study that proposed the formation of a mobile phase of AB during the induction period at 90 °C.[12] The NMR study further suggested that isomerization of AB to the diammoniate of diborane (DADB or $[(NH_3)_2BH_2]^+$ BH_4^-) is the critical nucleation event in the solid-state decomposition of AB. If true, the addition of a small amount of DADB or other chemical species to AB should lead to a significant reduction in the induction period.

In this paper, we discuss the important chemical pathways that lead to H_2 formation from solid AB. We report extensive isothermal calorimetric studies coupled with gas chromatography (GC) measurements of the yield of hydrogen as a function of time, illustrating the induction, nucleation, and growth phase that describe the dynamics of hydrogen release in solid AB. Further, we describe a combination of Raman spectroscopic studies of heat-treated AB crystals and time-dependent rate studies of hydrogen release from neat AB and AB doped with chemical additives using volumetric gas-measuring techniques. Additionally, we demonstrate the significant reduction in the induction time for hydrogen release from doped solid-state AB materials.

Experimental Section

Materials. AB (99%) from Aviabor was used without further purification for differential scanning calorimetry (DSC) and gas buret measurements. Ammonia borane can be prepared in high yields by a metathesis reaction between ammonium and borohydride salts.[13,14] Single crystals for Raman measurements were prepared by subliming AB onto a glass coverslip positioned over the Raman microscope's heating stage. The diammoniate of diborane was synthesized according to procedures described in the literature and gave an XRD pattern reported in the literature.[15] $LiAlH_4$, BF_3: etherate, and anhydrous ether were purchased from Aldrich Chemical Co. and used without purification; NH_3 was purchased from Scott Specialty Gases and dried over metallic sodium. All chemical additives were handled in an inert atmosphere in oven-dried glassware. NH_4Cl and $NaBH_4$ (Aldrich) were dried at 100 °C under a vacuum.

Methods. The calorimetric investigations were performed in a Setaram DSC (model C 80) with a sample mass of approximately 100 mg. This instrument was running in the measurements-in-scanning (heating rates 1 K/min) mode and in the isothermal (70 to 90 °C) mode. Volumetric data were collected by coupling the C-80 calorimeter with a GC equipped with a thermal conductivity conductor detector (Agilent model 3000A Micro GC) for gas-volumetric measurements. Values of heat flow and the evolved hydrogen were recorded simultaneously.

The yield of hydrogen release from AB as a function of temperature was determined by quantitative GC analysis. The sample cells were fitted with a needle valve that could be closed to prevent exposure to the atmosphere. The samples were prepared in a glovebox under an inert atmosphere and transferred to the C-80 calorimeter where an argon gas line equipped with mass flow controllers was connected to a tee to open the cell to release the hydrogen and keep the contents under an inert atmosphere during the reaction.

Volumetric gas measurements were performed using a gas burette system. All burette experiments were performed in base-washed, oven-dried, round-bottom flasks fitted with a stir bar. NH_3BH_3 and additives were massed inside the flasks and sealed. The reactor flasks were attached to the burette system, evacuated, and then refilled with N_2 for a total of three cycles. The flask then was opened to the burette system and plunged to its neck into preheated oil. The stirring speed was held constant at 100 rpm.

Raman spectra were measured using a stage mounted on confocal microscope stage. A 50 power objective was used to image the sample, focus approximately 5 mW of 532 nm polarized excitation from a CW Nd:YAG diode laser to an approximate 5-μm spot size on to the sample, and collect the Raman scattered light. The AB samples consisted of clusters of elongated, needle-like crystals that were approximately 15−25 μm in width and up to hundreds of microns long. Video imaging of sample under laser illumination allowed precise location of the focused laser beam on the sample. The Raman scattered light was collected in backscattering geometry, passed through an analyzer crystal, and finally scrambled before being focused on the entrance slit of a JY 800 triple spectrometer with 1600 g/mm gratings. The entrance and exit slits were maintained at 150 μm, and the scattered light then was dispersed onto a liquid nitrogen cooled charged coupled device Ge detector. The detector was calibrated using Hg emission lines. The Raman spectrum of AB ranges from 600 to 3700 cm^{-1}, thus necessitating collection of the entire spectrum in seven segments of approximately 600 cm^{-1} each. The Raman signal was averaged for a minimum of 300 s for each segment. The peak positions and lineshapes of the resulting Raman spectra were analyzed using GRAMS/32, a commercially available software package. A full factor group analysis of vibrational spectra for both orthorhombic and tetragonal phase of AB is provided elsewhere.[16]

Results

Isothermal Gas Chromatography Measurements of Hydrogen Release. Figure 1 compares the time-dependent yield of hydrogen gas released from AB during a series of isothermal measurements taken in the 75 and 90 °C temperature range. Three results are notable: (1) at all temperatures investigated, there is a relatively long induction period (i.e., more than 10 h at 75 °C); (2) following the induction period, the kinetics of hydrogen release show sigmoidal behavior that is consistent with a nucleation and growth kinetic model; and (3) the higher the temperature, the more

(11) Bowden, M.; Autrey, T.; Brown, I.; Ryan, M. *Curr. Appl. Phys.* **2008**, *8*, 498.
(12) Stowe, A.; Shaw, W.; Linehan, J.; Schmid, B.; Autrey, T. *Phys. Chem. Chem. Phys.* **2007**, *9*, 1831.
(13) Shore, S.; Parry, R. *J. Am. Chem. Soc.* **1955**, *77*, 6084.
(14) Heldebrant, D. J.; Karkamkar, A.; Linehan, J. C.; Autrey, T. *Energy Environ. Sci.* **2008**, DOI:10.1039/b808865A.
(15) Shore, S.; Boddeker, K. *Inorg. Chem.* **1964**, *3*, 914–916.
(16) Hess, N.; Parvanov, V.; Bowden, M.; Mundy, C.; Kathmann, S.; Schenter, G.; Autrey, T. *J. Chem. Phys.* **2008**, *128*, 034508.

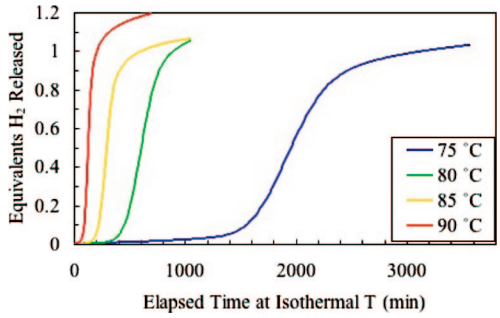

Figure 1. Isothermal H_2 release from NH_3BH_3 as a function of temperature illustrating the temperature-dependent induction period and yield of hydrogen release measured by gas burette.

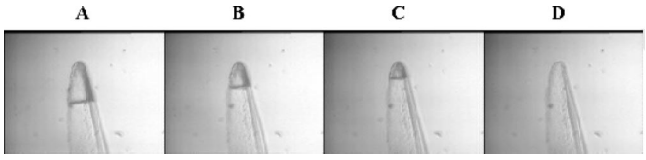

Figure 2. Optical micrograph images of a single crystal of NH_3BH_3 heated to 90 °C.

rapidly the reaction proceeds. The long induction period and sigmoidal kinetics are comparable to previous isothermal differential scanning calorimetry experiments.[3] At higher temperatures, slightly more than 1 equivalent of H_2 gas is released, and at lower temperatures, slightly less than 1 equiv of H_2 gas is released.

Raman Microscopy of Phase Transformation in Crystalline AB. Figure 2 shows a series of optical micrographic images of a single crystal of AB heated to 90 °C taken at various time intervals. A physical phase boundary is apparent; it moves toward the top of the frame as time progresses. Figure 3 shows the image of another AB crystal with a similar phase boundary that has been quench-cooled to room temperature after being heated to 90 °C.

A series of Raman spectra obtained above, through, and below the phase front at the locations indicated in Figure 3A are also shown in Figure 3B. Ahead of the phase front, top of the crystal at point [1], the Raman spectrum is that observed for crystalline AB: a strong B−N stretch at 785 cm^{-1}, B−H stretch at 2280 cm^{-1}, and N−H stretch at 3250 cm^{-1}.[16] As the Raman spectrum is taken closer to the phase front, these sharp peaks appear to broaden significantly, and finally below the phase front [5], a new vibrational frequency shifted to the higher energy of the observed B−H symmetric and asymmetric stretching frequency of AB. The higher frequency B−H stretching mode is observed in the Raman spectrum of an authentic sample of DADB.[17]

Gas burette measurements of hydrogen release in the presence of chemical additives. Figure 4 compares the time-dependent release of hydrogen from AB and AB doped (5 wt % dopant) with various additives as a function of time at 80 °C. The induction period for the initial release of hydrogen in neat AB (ca. 400 min) is significantly reduced with DADB present in the solid AB. For comparison, NH_4Cl and $NaBH_4$ were added as dopants to neat AB. While there is little notable effect in the induction period for hydrogen release in the presence of borohydride anion, there is a significant effect in the induction period for hydrogen production in the presence of the hydrochloride salt of ammonia.

^{11}B NMR Spectroscopy of Products Resulting from Hydrogen Release from AB. The solid-state ^{11}B NMR (17 T) spectra of AB heated to 85 °C for 600 min is shown in Figure 5. The ^{11}B NMR provides a qualitative diagnostic in to the basic structural features in polyaminoborane (PAB) formed by hydrogen loss from AB. In general, the further downfield the resonance, the less hydrogen there is attached to sp^3 type boron. Several boron structural features are observed in PAB: $BH(N_3) \approx -5$ ppm; $BH_2(N_2) \approx -12$ ppm; $BH_3(N) \approx -23$ ppm; $BH_4 \approx -40$ ppm; and sp^2 boron in polyborazylene approximately +25−30 ppm.

Discussion

The time dependence of hydrogen release at temperatures below the melting point of AB is indicative of a mechanism of hydrogen release from solid-state AB that occurs by a process involving (1) induction, (2) nucleation, and (3) growth. At temperatures below 100 °C, the induction period significantly curtails the onset of hydrogen release from solid AB. Understanding the chemical and physical processes occurring during the induction period leading up to the formation of the critical nucleation event is essential to enhancing the rates of hydrogen release from AB. Nucleation in AB could be a physical change in the material, creation of defects in the solid AB material, or some chemical change; for example, the formation of a more reactive chemical species, the initial coupling product, a linear dimer, or formation of DADB could be the critical nucleation event.

The optical micrographs (Figure 3A) show a moving phase front in a crystal of AB heated to 90 °C. Raman spectroscopy shows a change from the well-resolved bands of crystalline phase AB to less-well-resolved signals as the spectra are measured across the phase boundary. The less well-resolved signals are characteristic of what would be expected in an amorphous phase of AB. Finally, DADB is observed further on the opposite side of the phase front in addition to the amorphous AB. The appearance of DADB before hydrogen is released is consistent with the observation of DADB in the in situ ^{11}B NMR studies[12] and provides further evidence of the formation of DADB as the nucleation event. These results also are consistent with previous in situ XRD results[11] that show a conversion of crystalline AB to an amorphous phase and provide further evidence for the enhanced probability of isomerization of AB to DADB as the dihydrogen bonding network is disrupted.

A direct correlation exists between the spectroscopic observation of DADB formed at the end of the induction period and the spectroscopic observation of the PAB-like products that arise from the release of hydrogen. While this could be interpreted as evidence for DADB as the nucleation event leading to hydrogen release from solid AB, we can not rule out either (1) another minor unobserved species or (2) a physical change in the crystalline phase occurring concurrent with DADB formation from amorphous AB. However, if formation of DADB is the critical nucleation

(17) Taylor, R.; Schultz, D.; Emery, A. *J. Am. Chem. Soc.* **1958**, *80*, 27–30.

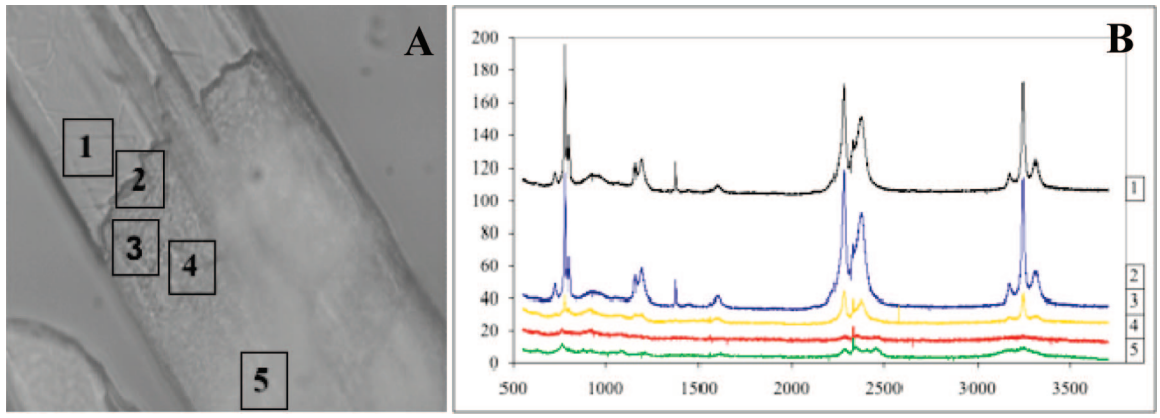

Figure 3. (A) Optical micrograph image of a single crystal of NH_3BH_3 that has been quench-cooled to room temperature after being heated to 90 °C heated to 90 °C shows a similar phase boundary as observed in Figure 2. The corresponding Raman spectra taken at the corresponding numbered sites shows that from top to bottom,the crystalline AB becomes amorphous and isomerization to DADB is observed.

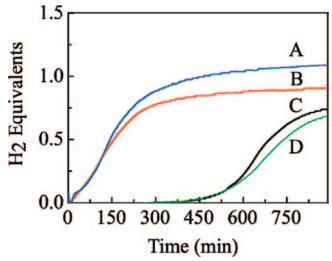

Figure 4. Effect of additives on the induction period for H_2 release from solid AB at 80 °C. (A) NH_3BH_3:NH_4Cl (5 wt %), (B) NH_3BH_3:DADB (5 wt %), (C) NH_3BH_3, (D) NH_3BH_3:$NaBH_4$ (5 wt %).

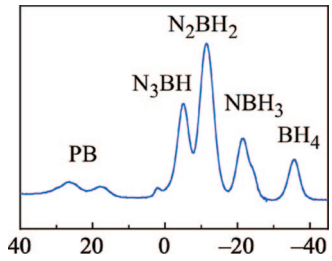

Figure 5. ^{11}B MAS NMR of NH_3BH_3 heated to 85 °C for 10 h resulting in the loss of 1 equiv of hydrogen. The product(s), PAB, are a complex material containing several boron environments in addition to N_2BH_2.

event, the addition of a small amount of DADB to crystalline AB should significantly reduce the induction period. To test this hypothesis, we prepared an authentic sample of DADB and measured the induction period for hydrogen evolution from neat AB and AB doped with 5 wt % DADB. As shown in Figure 3, the presence of a small quantity of DADB significantly decreases the induction period for hydrogen release from solid-state AB.

Literature reports suggest that the two isomers (AB and DADB) may be sufficiently close in energy to exist in equilibrium. However, the evidence is quite ambiguous with some reports suggesting AB slowly isomerizes to DADB, and other reports suggesting DADB slowly isomerizes to AB at room temperature.[18–20] Calculations comparing the relative energies of an AB dimer and DADB suggest that DADB is less stable than AB.[21,22] These modeling results, combined with our present observations, led us to propose that heating AB disrupts the dihydrogen bonding network and permits a transition-state structure that yields the isomerization of AB to DADB with no loss in hydrogen. The formation of DADB is the "nucleation" step followed by "growth" or hydrogen release that arises from a fast reaction between DADB and AB.

While the results discussed above are consistent with this model for hydrogen release, they do not provide insight into what "functionality" of DADB makes it more reactive with AB. Further insight into the chemical nucleation process may be gained from the time dependence of hydrogen release in the presence of other chemical additives that test the molecular functionality of hydrogen release. Because DADB is composed of an boronium cation $[NH_3BH_2NH_3]^+$ and a borohydride anion $[BH_4]^-$, experiments can be devised to investigate these individual functional groups. It is feasible that either ion could react with AB at a rate faster than AB reacts with itself. The gas burette experiments showing the time-dependent release of hydrogen in the presence of NH_4Cl and $NaBH_4$ provide a direct insight into the initial reaction pathways leading to hydrogen release from solid-state AB. The results clearly show that the NH_4Cl decreases the induction period, whereas the $NaBH_4$ has little measurable effect. This is an important finding because it not only shows that it is the cation that has a rate-determining role, but that hydrogen release rates can be significantly enhanced by the addition of a small amount of NH_4Cl to AB.

The release of hydrogen from solid AB has been described in the past by a relatively simple stepwise mechanistic pathway (see eqs 1a and 2a below). However, ^{11}B NMR data of the products formed after the release of 1 equivalent of hydrogen suggest that the pathways releasing hydrogen are more complex with competing cross-linking (eq 1c) steps that also contribute to the observed hydrogen yields at temperatures below 100 °C. The ^{11}B NMR spectra shown in Figure 4 show that the PAB product formed after heating AB to 85 °C for 10 h is composed of $B(H)N_3$, $BH_2(N_2)$,

(18) Mayer, E. *Inorg. Chem.* **1973**, *8*, 1954–1955.
(19) Shore, S.; Parry, R. *J. Am. Chem. Soc.* **1958**, *80*, 8–12.
(20) Parry, R. *J. Chem. Educ.* **1997**, *74*, 512–518, and references therein.
(21) Smith, R.; Kay, B.; Li, L.; Schmid, B.; Hess, N.; Gutowski, M.; Autrey, T. *Abstr. Pap. Am. Chem. Soc.* **2005**, *229*, U858.
(22) Nguyen, V.; Matus, M.; Grant, D.; NguyenM.; Dixon, D. *J. Phys. Chem. A* **2007**, *111*, 8844–8856.

$BH_3(N)$, and BH_4. Unfortunately, the resolution in the ^{11}B solid-state NMR spectra is not sufficient to identify products such as B-(cyclodiborazanyl) aminoborohydride, *cyc*[NH_2BH_2-NH_2BH]-NH_2BH_3 (BCBD) that were recently reported to be important in the solution phase decomposition of AB.[23] The BH_4 resonance results from the isomerization of AB to DADB (eq 1b) and the corresponding products (eq 1d).

We believe NH_4Cl overcomes the induction period through the formation of $[(NH_3)_2BH_2]^+Cl^-$,[24] which possesses the same cation as DADB. Preliminary experiments have confirmed that NH_4Cl and AB react at 80 °C to form $[(NH_3)_2BH_2]^+Cl^-$ and H_2 gas. The reaction then proceeds by a similar pathway as described in eq 1d with an analogous product (i.e., $[NH_3BH_2NH_2BH_2NH_3][Cl]$). This proposal is supported by ^{11}B NMR spectra of the products after hydrogen loss (Supporting Information) that shows a similar distribution of boron environments with and without seeding. Seeding with NH_4Cl yielded less BH_4^- in the product, which is consistent with the presence of the chloride counterion. Further work is in progress to define the reaction mechanisms. The additional cross-linking reactions give rise to $B(H)N_3$ resonances observed to be approximately −5 ppm. This mechanism, which involves chain growth from ionic isomers and cross-linking, also has been observed for hydrogen release from methylamine borane.[25,26]

$$NH_3BH_3 \rightarrow (NH_2BH_2) + H_2 \quad <100\ °C \qquad (1a)$$

$$2NH_3BH_3 \rightarrow [NH_3BH_2NH_3][BH_4] \quad <100\ °C \qquad (1b)$$

$$2(NH_2BH_2)_n \rightarrow (NH_2BH - NHBH_2)_n + nH_2 \quad <100\ °C \qquad (1c)$$

$$DADB + AB \rightarrow [NH_3BH_2NH_2BH_2NH_3][BH_4] + H_2 \quad <100\ °C \qquad (1d)$$

The loss of the second equivalent of hydrogen from AB by the intramolecular pathways described by eq 2a does not contribute significantly to the hydrogen formation at temperatures less than 100 °C because there is little sp^2 boron (polyborazylene) detected by ^{11}B NMR. This is in contrast to the behavior of lithium amidoborane, $LiNH_2BH_3$, which loses 2 equiv of H_2 at 90 °C to yield a polyborazylene-like species as the major product observed by ^{11}B NMR spectroscopy.[27]

$$(NH_2BH_2) \rightarrow (NHBH) + H_2 \quad >100\ °C \qquad (2a)$$

$$2(NHBH) \rightarrow (NHB-NBH) + H_2 \quad >150\ °C \qquad (2b)$$

Conclusions

The induction period for the onset of hydrogen release from AB involves the disruption of the dihydrogen bonding network to form an amorphous phase of AB. In the amorphous phase, AB isomerizes to DADB, which reacts rapidly with AB to release hydrogen and yield a highly branched PAB oligomer.

This work shows that the induction period for the release of hydrogen can be significantly reduced by seeding pure samples of AB with a solid acid such as DADB or NH_4Cl. The ability to reduce the induction period solves one of the major technical hurdles for considering AB as a chemical hydrogen storage material for fuel-cell-powered vehicles.

Acknowledgment. The authors acknowledge support from the U.S. Department of Energy's Office of Energy Efficiency and Renewable Energy. This work was performed as part of the Center of Excellence in Chemical Hydrogen Storage and in collaboration with the International Partnership for the Hydrogen Economy. Pacific Northwest National Laboratory is operated for the Department of Energy by Battelle. A portion of the research described in this paper was performed in the W.R. Wiley Environmental Molecular Sciences Laboratory, a national scientific user facility sponsored by the Department of Energy's Office of Biological and Environmental Research and located at Pacific Northwest National Laboratory.

CM801253U

(23) Shaw, W. J.; Linehan, J. C.; Szymczak, N. K.; Heldebrant, D. J.; Yonker, C.; Camaioni, D. M.; Baker, R. T.; Autrey, T. *Angew. Chem., Int. Ed.* **2008**, in press.
(24) Nordman, C.; Peters, C. *J. Am. Chem. Soc.* **1959**, *81*, 3551–3554.
(25) Beachley, O. *Inorg. Chem.* **1967**, *6*, 870.
(26) Bowden, M.; Brown, I.; Gainsford, G.; Wong, H. *Inorg. Chim. Acta* **2008**, *361*, 2147–2153.
(27) Xiong, Z.; Yong, C.; Wu, G.; Chen, P.; Shaw, W.; Karkamkar, A.; Autrey, T.; Jones, M.; Johnson, S.; Edwards, P.; David, W. *Nat. Mater.* **2008**, *7*, 138–141.